Contents lists available at ScienceDirect

Environment International

journal homepage: www.elsevier.com/locate/envint

# Demonstrating the translocation of nanoplastics across the fish intestine using palladium-doped polystyrene in a salmon gut-sac

Nathaniel J. Clark [a,*], Farhan R. Khan [b,c], Denise M. Mitrano [d], David Boyle [a,e], Richard C. Thompson [a]

[a] School of Biological and Marine Sciences, University of Plymouth, Plymouth PL4 8AA, UK
[b] Norwegian Research Centre (NORCE), Nygårdsporten 112, NO-5008 Bergen, Norway
[c] Department of Science and Environment, Roskilde University, Universitetsvej 1, PO Box 260, 4000 Roskilde, Denmark
[d] Department of Environmental Systems Science, ETH Zurich, 8092, Switzerland
[e] Cobalt Institute, 18 Jeffries Passage, Guildford GU1 4AP, UK

ARTICLE INFO

Handling Editor: Martí Nadal

*Keywords:*
Plastic nanoparticle
Gut
Gastrointestinal tract
Intestine
Uptake

ABSTRACT

Fish are widely reported to ingest microplastics with low levels accumulating in the tissues, but owing to analytical constraints, much less is known about the potential accumulation of nanoplastics via the gut. Recently, the labelling of plastics with inorganic metals (e.g., palladium) has allowed measurements of nanoplastic uptake. The aim of the current study was to quantitatively assess the uptake of nanoplastics by the fish gut using palladium-doped nanoplastics (with a mean hydrodynamic radius of 202 ± 7 nm). By using an *ex vivo* gut sac exposure system, we show that in 4 h between 200 and 700 million nanoplastics (representing 2.5–9.4% of the administered nanoplastics dose) can enter the mucosa and muscularis layers of the intestine of salmon. Of the particles taken up, up to 700,000 (representing 0.6% of that taken into the tissue) of the nanoplastics passed across the gut epithelium of the anterior intestine and exit into the serosal saline. These data, generated in highly controlled conditions provide a proof-of-concept study, suggesting the potential for nanoplastics to distribute throughout the body, indicating the potential for systemic exposure in fish.

## 1. Introduction

Plastics are ubiquitously present in the environment (Barnes et al., 2009) and are considered a hallmark of the Anthropocene (Zalasiewicz et al., 2016). Microplastics (nominally < 5 mm (Arthur et al., 2009)) and nanoplastics (<1 μm (Kershaw, 2015) or < 0.1 μm (Chain, 2016) depending on the definition used) can be directly released into the environment or formed from the degradation of larger plastic items (Koelmans et al., 2015). The ingestion of microplastics has been reported for a variety of aquatic organisms including zooplankton, polychaetes, bivalves, fish, birds and mammals (Phuong et al., 2016), but the majority of such research has focused on fish species. Microplastics have been found in the gastrointestinal tracts of fish around the world (Azevedo-Santos et al., 2019), but the fate of ingested particles and the potential for them to be transferred from fish to higher trophic levels remains unclear. Particulates in the intestine achieve cellular internalization via endocytotic processes which conventionally have a size limitation in the low micron size range (Mitrano et al., 2021). Thus, microplastics are unlikely to pass into the tissue, although recent studies suggest cellular uptake may be enhanced by surface functionalisation and environmental transformations, such as the formation of eco-coronas (Ramsperger et al., 2020). From the perspective of human consumption, most species are consumed after removing the gastrointestinal tract, the presence of microplastics within fish intestines has not led to significant human health concerns (Lusher et al., 2017). Nanoplastics present a different proposition (Gigault et al., 2021); endocytotic mechanisms of plastic particles are possible in the nano-size range which may translocate into parts of the fish that are consumed. To date, clear demonstrations of nanoplastic uptake across the fish intestine are absent from the literature. Furthermore, the relative amount of nanoplastics capable of crossing the intestinal membrane is unknown but is a vital knowledge gap if the toxicological risks of nanoplastics are to be understood.

Research on the uptake and distribution of nanoplastics in aquatic organisms has intensified in recent years (Shen et al., 2019), but the detection of carbon-based polymers against a high carbon background

* Corresponding author.
*E-mail address:* nathaniel.clark@plymouth.ac.uk (N.J. Clark).

https://doi.org/10.1016/j.envint.2021.106994
Received 20 September 2021; Received in revised form 15 November 2021; Accepted 17 November 2021

remains a significant analytical challenge within biological samples. Employing fluorescent labels to trace nanoplastics necessitates the use of fluorophores which may leach from the particle or tissues may emit autofluorescence, rendering results inconclusive (Catarino et al., 2019). Using conservative tracers entrapped within the particle during synthesis negates such concerns (Al-Sid-Cheikh et al., 2020; Mitrano et al., 2019) and allows a quantitative assessment of uptake potential. Here, we used nanoplastic particles synthesized with chemically entrapped palladium (Pd) (Mitrano et al., 2019) which allows for the detection and quantification of particle uptake via analysis of the tissue Pd burdens.

The aim of the present study was to determine whether nanoplastics are bioavailable in the gut of fish, and establish which intestinal region nanoplastic uptake would occur. The palladium-doped nanoplastics (PS-Pd NPs) were utilised in combination with an *ex vivo* gut sac experiment that is an established method to study the transport processes in fish gastrointestinal tracts. This technique has been used to understand the uptake of dissolved trace metals (Bury et al., 2001; Ojo and Wood, 2007), engineered metal-containing nanomaterials (Boyle et al., 2020b; Clark et al., 2019b) and to determine the role of microplastics as a vector for pollutants (Khan et al., 2017). The basis of the technique is the ongoing viability of gastrointestinal tissue following its excision from the fish. The gastrointestinal tract can be divided into three functional regions, anterior-, mid and hind- intestine into which physiological saline containing the compounds of interest can be directly introduced within the gut lumen (Fig. 1). The sealed gut sac is then incubated for a short period of time before analysing the distribution of the test substance between the layers of the gut tissue, namely the gut lumen, mucosa, muscularis and serosal saline, with the last layer representing uptake into the blood compartment. In this study, we used the gut sac technique for the first time to demonstrate the capacity of nanoplastic uptake from fish gastrointestinal tracts.

## 2. Materials and methods

### 2.1. Animal husbandry

Throughout this work, salmon (*Salmo salmar*) were used as an established model species in ecotoxicology, their importance in the aquaculture industry and relevance to human consumption, and ability to breach freshwater and marine habitats, enabling results to be applicable to both environments. The use and care of animals in this study was in line with institutional guidelines and underwent internal ethical approval prior to starting (reference number ETHICS-43–2020). Freshwater adapted salmon (*Salmo salmar*) weighing 107.8 ± 19.9 g (n = 16, mean ± S.D.) were obtained from Landcatch Natural Selection Ltd fish farm and held in a recirculating system at the University of Plymouth. Prior to experimental use, fish were acclimated to local conditions (e.g., dechlorinated Plymouth tap water) for 7 days and fed twice a day with commercially available fish feed. Fish were maintained under the following water quality parameters (mean ± S.D., n = 4) for pH (6.95 ± 0.07), dissolved oxygen (9.39 ± 0.04 mg $L^{-1}$) and temperature (17.48 ± 0.29 °C). Additional water samples were taken on experimental days to measure the total palladium concentration in the aquarium water. The water total palladium concentration were below the limit of detection of the ICP-MS (10 ng $L^{-1}$).

### 2.2. Synthesis of palladium-doped nanoplastics

The palladium-doped nanoplastics (PS-Pd NPs) used in the present work were synthesised according to Mitrano et al. (2019). Briefly, a two-step emulsion polymerization in which first the particle core was synthesized (which contained the metal), after which a further shell of polystyrene was grown through feeding a second monomer-containing solution over time to augment the surface chemistry and morphology of the original particle. For the nanoplastic core, the surfactant (SDS) and initiator were charged inside the reactor with the monomer (acrylonitrile). When the initial nucleation point was achieved, the dissolved metal precursor was added slowly over the course of five minutes to the reaction vessel. The evolution of the polymer conversion and particle size were followed through dynamic light scattering (DLS) (Malvern Zetasizer Nano Z, backscatter angle 173° at 25 °C) and thermogravimetric analysis (TGA) at T = 120 °C (Mettler Toledo), respectively. After a conversion rate of approximately 90% was achieved, the shell feed was directly plumbed into the reaction vessel along with an additional shot of initiator and water. The shell feed, a mixture of water, styrene, DVB and SDS, was dosed for 4 h. The particle growth and extent of conversion was again closely monitored with samples collected every half hour to follow the reaction progress. The nanoplastics were stored at room temperature and in the dark.

### 2.3. Nanoplastic characterisation

Spherical PS-Pd NPs were characterized prior to use in the exposure studies in terms of metal content and particle size (see Mitrano et al., 2019 for full details). Briefly, the primary stock suspension was diluted 100-fold using high purity water, and 0.1 mL of this stock was digested in 3 mL of acid (3:1 $HNO_3$:HCl). The mixture was left at room temperature for 1 h before being placed onto a hot plate and carefully bought to

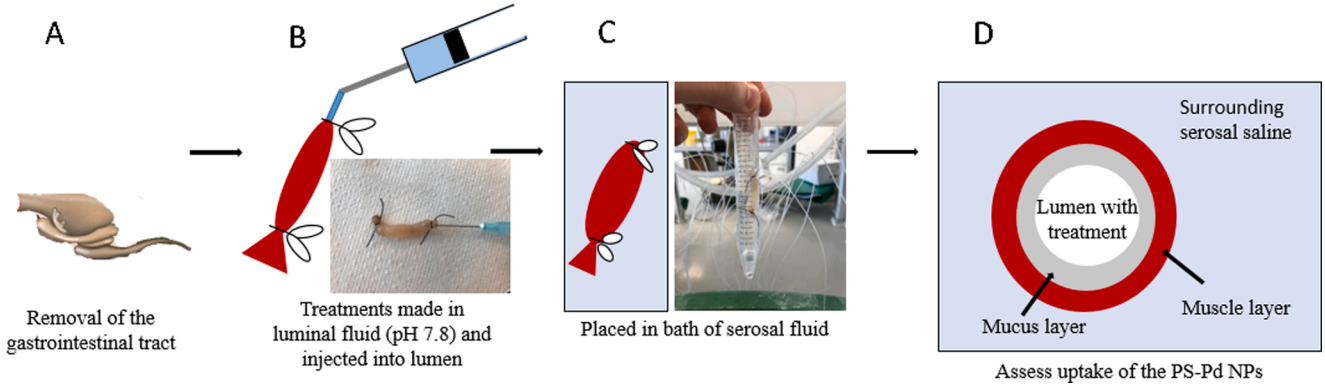


**Fig. 1.** Schematic of the gut sac technique. (A) The entire gastrointestinal tract is removed from the fish and separate gut sacs were made for each anatomical region (anterior intestine [including the pyloric caeca], mid intestine and hind intestine. (B) The PS-Pd NPs are added to the gut lumen to assess their uptake. (C) The gut sac is closed and incubated in the serosal compartment for 4 h. (D) At the end of the experiment, the gut sac is cut open, rinsed and the mucosa is separated from the muscularis using a glass microscope slide, and measured for total Pd measurements. The gut cross section shows the different tissue layers, highlighting the gut lumen (white), mucosa (grey) and muscularis (red). The serosal saline is analysed for the presence of particles using single particle ICP-MS. (For interpretation of the references to colour in this figure legend, the reader is referred to the web version of this article.)

a simmer. The samples were left for the digestion to complete (i.e., no brown fumes and producing a final colourless solution) and further diluted before analysis using inductively coupled plasma mass spectrometry (iCAP RQ ICP-MS, Thermo Fisher). The measured total Pd concentration was 255.8 ± 3.9 mg Pd $L^{-1}$ (mean ± S.D, n = 3), and this concentration was used for subsequent dosing. Particle hydrodynamic diameter was determined by Nanoparticle Tracking Analysis (LM10, Malvern, UK) in Fig. 2. The mean particle size was determined as a hydrodynamic diameter of 202 ± 7 nm when PS-Pd NPs were dispersed in ultrapure water and increased to 228 ± 6 nm (mean ± S.D, n = 3) when dispersed in physiological gut saline (Fig. 2).

The release of $Pd^{2+}$ from the PS-Pd NPs during the exposure would have presented a confounding factor in determining particle uptake since the presence of the ionic form would indicate tissue concentrations were not from the presence of particles, but diffusion of ions. Therefore, to quantify the presence of dissolved palladium, a dialysis experiment was performed in physiological gut saline to mimic the gut environment (in mmol $L^{-1}$: NaCl, 117.5; KCl, 5.7; $NaHCO_3$, 25.0; $NaH_2PO_4{\cdot}H_2O$, 1.2; $CaCl_2$, 2.5; $MgSO_4{\cdot}7H_2O$, 1.2; glucose, 5.0; mannitol, 23.0; pH 7.8 (Clarket al., 2019b)). A 50 mg $L^{-1}$ Pd stock of the PS-Pd NPs was made,

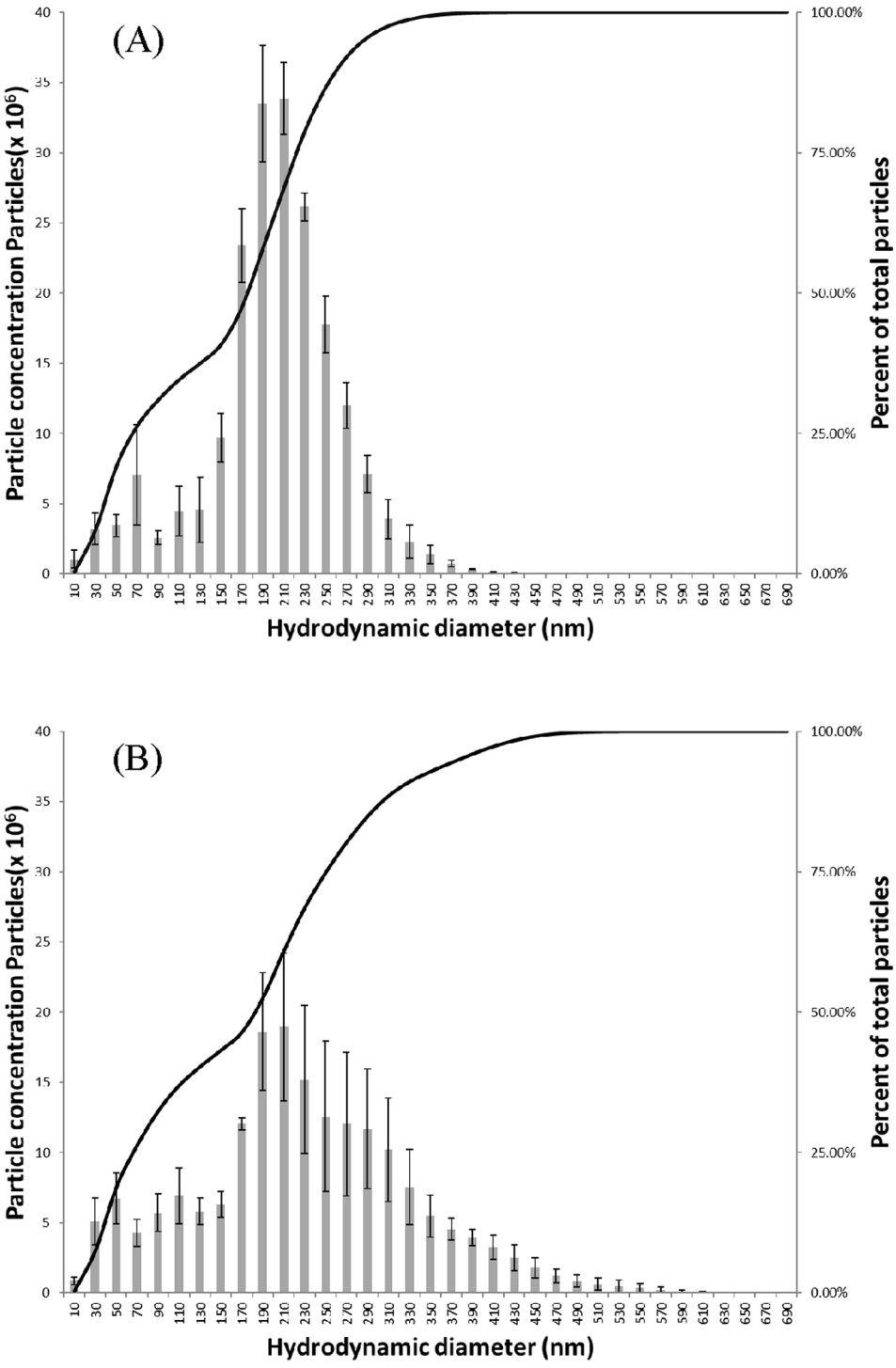


**Fig. 2.** PS-Pd NP hydrodynamic diameter and particle number concentration in (A) high purity water or (B) physiological gut saline. Data are mean ± S.D., n = 3. Note the increased presence of higher bin sizes in (B).

of which 3 mL was added to the dialysis tubing which was tied at both ends. The filled dialysis bag was then placed in 297 mL of physiological gut saline. The presence of $Pd^{2+}$ outside the dialysis bag was measured over the 4 h period with 0.5 mL samples taken at 0, 0.25, 0.5, 1, 2 and 4 h. Samples were acidified with $HNO_3$ and HCl (3:1), and further diluted to a final volume of 2.5 mL prior to analysis by ICP-MS for total Pd concentration. The instrument limit of detection was $0.032 \pm 0.004$ ng Pd $mL^{-1}$.

### 2.4. Ex vivo gut sac experiment

Fish were euthanized according to institutionally approved methods, of induced concussion and pithing (Schedule 1, in accordance with ethical approvals, Home Office, UK, and in compliance with the EU directive 2010/63/EU), and the entire gastrointestinal tract was removed from buccal cavity to anus (Fig. 1). The intestines are the predominant site of absorption; therefore, these were the areas of focus. The three intestinal regions of the gastrointestinal tract (anterior intestine (including the pyloric caeca), mid intestine and hind intestine) were carefully separated into individual compartments, and the gut lumen rinsed using physiological gut saline to remove any residual food/material. The weight of each empty gut sac was recorded, and sutured closed at one end. Each gut sac was then filled with gut physiological saline (pH 7.8) containing one of two treatments: saline only (control) or PS-Pd NPs (total Pd concentration of 1 μg $mL^{-1}$, equivalent to 1.03 x$10^{10}$ particles [as calculated by spICP-MS, see below], n = 6 per treatment). This concentration of PS-Pd NPs was used to allow comparison to other materials that have been assessed in the same manner (e.g., Clark et al., 2019b), and ensure that, if bioavailable, the signal could be detected in the tissue. The opposite end of the gut sac was then sutured shut and re-weighed to calculate the volume of saline added to allow for calculations on the percentage of PS-Pd NPs taken into the tissue. The exterior of the gut sacs were then rinsed using clean physiological gut saline, and placed in 20 mL (anterior intestine) or 7.5 mL (mid intestine and hind intestine) of clean physiological gut saline. Each tube was in a water bath kept at 15 °C degrees, and individually gassed using 99.7:0.3% $O_2$:$CO_2$ for 4 h (Fig. 1).

Following the 4 h exposure (i.e., the length of time that an *ex vivo* gut sac maintains viability and functionality (Al-Jubory and Handy, 2013)), the gut sacs were removed from the tubes, and excess moisture was removed prior to being re-weighed. To measure fluid movement from the mucosal to the serosal compartments, or vice-versa, the difference in weight before and after the treatments was assessed gravimetrically. The gravimetric method has been determined to be the most reliable method of measuring fluid transport (Whittamore et al., 2016). The test tubes containing the serosal saline were stored at −20 °C until analysis by single particle ICP-MS. Each gut sac was carefully cut open and rinsed in 5 mL of clean gut physiological saline to remove material loosely bound to the surface of the gut epithelium. The gut sac was then immediately rinsed in a second rinse of gut physiological saline with 1 mmol $L^{-1}$ EDTA. This process has been shown to be efficient at removing > 95% of surface bound particles (Clark et al., 2019b). While EDTA is added to the second wash step, its main purpose is to remove any surface bound metals (Clark et al., 2019b); here, the Pd is encapsulated in the polymer, but is used regardless for the whole procedural efficiency remained high (see Surface binding experiment below), meaning any Pd found in the tissues reflects material accumulated. To separate the tissues, a microscope slide held at a 45-degree angle and carefully dragged across the piece of gut tissue, removing the surface mucosa from the underlying muscularis (Fig. 1). The exception to this is the anterior intestine, where the caeca cannot be reliably emptied of added saline and/or PS-Pd NPs (see Clark et al., 2019b). Therefore, only the anterior intestine tissue of this gut region was taken for analysis. Then, both the mucosa and muscularis were weighed before being stored at −20 °C. The tissues were then freeze dried, re-weighed (for tissue moisture calculations) and digested prior to total Pd measurements.

### 2.5. Surface binding experiment

To quantify the efficiency of the rinse solutions (physiological saline + EDTA, as above) in removing any loosely bound surface PS-Pd NPs, a rapid solution dipping experiment according to Clark et al. (2019b) was performed. Only the mid and hind intestine regions were selected for this due to their ease of inversion so they can be dipped into a suspension of PS-Pd NPs to quantify adsorption to the mucosa. Everted intestinal segments were sutured shut to prevent any PS-Pd NPs from being exposed to the muscularis and ensuring only the mucosa is exposed. Both the mid and hind intestines were rinsed in gut physiological saline (as above) and then dipped into a suspension of 1 μg $mL^{-1}$ PS-Pd NPs (to reflect those in the main experiment) for 30 s. This duration is to mimic exposure of the mucosa, but does not allow for any instantaneous uptake (Al-Jubory and Handy, 2013). Tissues were then removed and treated as above prior to measurements of total Pd concentrations.

### 2.6. Gastrointestinal tissue total palladium concentration

In the absence of an appropriate certified reference materials for total palladium in tissues, a series of spike and recovery tests were used to ensure the digestion protocol was sufficient to recover all Pd. Control tissues were obtained from additional fish (n = 3), and the anterior intestine, mid intestine and hind intestine removed. These tissues were frozen, dried and weighed, as discussed above. In glass vials, tissues were added to 2.25 and 0.75 mL nitric acid and hydrochloric acid, respectively. In addition, 50 μL of a 2.55 mg $L^{-1}$ Pd as PS-Pd NPs was also added. The samples were allowed to digest at room temperature for 1 h, before being slowly heated on a hot plate to simmering point (~100 °C). The samples were then left until they were completed (i.e., production of a colourless liquid and absence of fumes) before being allowed to cool to room temperature. Following this, each sample was diluted to 15 mL and spiked with indium and iridium (to give a final concentration of 20 μg $L^{-1}$) for use as an internal standard to monitor instrument drift during analysis by ICP-MS. Tissue total Pd concentrations were compared to matrix matched standards and during the analysis a check standard was analysed every 10–12 samples. Between each sample, a 2% nitric acid solution was used to remove cross contamination from the sample introduction system. The recovery of the PS-Pd NPs in the presence of the different tissues was compared to the PS-Pd NPs alone (i.e., no tissue). The recovery rates for the anterior intestine mucosa, anterior intestine muscularis, mid intestine mucosa, mid intestine muscularis, hind intestine mucosa and hind intestine muscularis were 98.6 ± 1.8, 98.0 ± 4.4, 98.9 ± 2.4, 95.9 ± 3.2, 95.8 ± 1.6 and 97.3 ± 5.7 %, respectively. Given the high recovery rates of Pd, all experimental samples from the gut sac and surface binding experiment were processed in the exact same process.

### 2.7. Measurement of PS-Pd NPs and the serosal compartment using single particle ICP-MS

The use of single particle ICP-MS had two roles; firstly, to determine the number of particles in a given mass to calculate the number of particles in the tissue. To achieve this, the stock suspension was diluted to an appropriate mass concentration, using ultrapure water, and analysed by spICP-MS (as below). The output is the number of particles present in the aspirated suspension (i.e., a known mass concentration). From this, the number of particles for the given mass was used to calculate the number of particles in the PS-Pd NP exposed tissues (i.e., with a known mass of Pd). The second aim was to determine the number of particles in the serosal saline of the PS-Pd NP exposed gut sacs. The serosal saline represents part of the blood compartment, but detecting low levels of total Pd in the serosal compartment using ICP-MS following digestion is difficult due to high salt concentrations and expected low metal concentrations which may be near or below analytical detection

limits. To avoid these drawbacks of total Pd analysis, the investigation of PS-Pd NP presence in the serosal saline was conducted using single particle ICP-MS. The serosal salines from the gut sac experiments were thawed and diluted 5-fold with ultrapure water to give a final volume of 2 mL. The samples were then analysed using single particle ICP-MS.

The single particle ICP-MS analysis was performed according to Clark et al. (2019c) with minor modifications. An iCAP RQ ICP-MS was operated in collision cell mode with He as the cell gas. For sample introduction, a micromist nebuliser and quartz cyclonic spray chamber cooled to 2 °C was used. The instrument plasma power was set at 1550 Watts. The plasma, nebulizer and auxiliary Ar flow rates were 14.0, 1.0 and 0.8 L $min^{-1}$, and nickel plated sampler and high matrix skimmer cones were used. A dwell time of 3 ms was used in all analysis, and samples were analysed for 60 s. Prior to analysis, the instrument was tuned using a multi-element standard, with the indium signal used for optimal stability and sensitivity and a minimum oxide (CeO/Ce) formation of < 0.01%. Only one *m/z* ratio can be monitored at a time, and so $^{105}$Pd was selected. Between samples, a 2% nitric acid wash solution was used to reduce sample cross contamination from the sample introduction system. The flow rate of the instrument was calculated gravimetrically before use by difference between uptake of ultrapure water over 2 mins (n = 5) and was 0.3 mL $min^{-1}$. The transport efficiency was also calculated prior to use (according to Pace et al., 2011). To calculate the transport efficiency, Au NPs were diluted to match the matrix of the samples and analysed. A series of dissolved standards were made between 0 and 0.25 μg $L^{-1}$. The standards were analysed at the start of the analysis, and then checked throughout after 9–10 experimental samples. The data was then exported and handled in a bespoke Excel spreadsheet (see Peters et al., 2014 for details) to calculate the particle mass concentration and the particle number concentration. All solution/suspension preparation and analysis were performed in a laboratory managed under an ISO9001 certified quality management system.

### 2.8. Statistics and calculations

All results are presented as mean ± SEM, unless otherwise stated. The distribution of PS-Pd NPs through the tissue layers was calculated through the sum of Pd in the mucosa, muscularis and serosal saline, and expressing each compartment as function of total Pd in all combined compartments. Statistical analysis and graphs were conducted in SigmaPlot 13.0. Data sets with suspected outliers were checked for normality (Shapiro-Wilk, $P > 0.05$) and, having passed this were then analysed using Grubbs test ($P < 0.05$). Subsequently, all results were then checked for normality and equal variance (Brown-Forsythe test). Normally distributed data, or those that could be $\log_{10}$ transformed to a normal distribution, were analysed using a one-way ANOVA (for gut region differences [tissue Pd concentrations, number of particles in tissues and relative amount of Pd absorbed], or treatment effects [fluid flux and moisture content]). For non-normal data, and data that could not be transformed to a normal distribution, the Kruskal-Wallis test was used. Each test was followed by a post hoc Tukey's or Dunn's test, and the individual *P* values presented are from the post hoc tests.

## 3. Results

### 3.1. PS-Pd NP behaviour in physiological gut saline

Various characterisation and validations were necessary to understand the behaviour of the nanoplastics in the simulated gut environment and to ensure that the Pd concentration found in gut tissue could only be attributed to presence of PS-Pd NPs. The mean hydrodynamic particle size was 202 ± 7 nm when PS-Pd NPs were dispersed in ultrapure water and increased to 228 ± 6 nm (mean ± S.D, n = 3) when dispersed in physiological gut saline (Fig. 2). The largest size category of particles found (as evidenced from NTA measurements, Fig. 2) was 610 nm, suggesting some aggregation of the particles occurred as would be expected in solutions with high ionic strength. The proportion at this size range remained small (<0.03%). The release of ionic $Pd^{2+}$ from the PS-Pd NPs within gut saline mimicking the conditions of the *ex vivo* gut sac experiment was determined with the use of a dialysis bag experiment. Only 0.08% of the ionic constituent was released. Furthermore, there was no detectable $Pd^{2+}$ in the control fish across all gut regions and tissue layers. Validating the negligible background Pd concentration in the test system provides further confidence that any Pd detected in the tissue layers following exposure to the nanoplastics was in the form of intact PS-Pd NPs that had translocated from the gut lumen. In addition, the surface binding experiment showed trace amounts of PS-Pd NPs instantaneously bound to the surface of the mucosa of the mid and hind intestine (50.9 ± 8.9 and 36.6 ± 1.6 ng $g^{-1}$ dw, respectively), ensuring the Pd signal was from internalised PS-Pd NPs. Such validation also extends to the viability of the gut sac preparations typically measured as fluid flux and tissue moisture. There was no significant difference between the control gut sacs (i.e. no added PS-Pd NPs) and the PS-Pd NP treatments for the anterior (one-way ANOVA, F = 0.103, DF = 1, $P = 0.818$), mid (one-way ANOVA, F = 0.007, DF = 1, $P = 0.937$) and hind intestine (one-way ANOVA, F = 1.362, DF = 1, $P = 0.270$). This ensures the presence of the PS-Pd NPs did not upset normal gastrointestinal function (Table 1).

### 3.2. Distribution of PS-Pd NPs throughout the gut sac

In all control tissue samples, there was no detectable Pd. In contrast, total Pd was found in all tissues of the PS-Pd NP exposed gut tissues, and in some serosal salines. Most of the particles taken up by the gut from the PS-Pd NP exposure were in the mucosa (>88%, Fig. 3), with some statistical difference between gut regions (Kruskal-Wallis, H = 9.722, DF = 2, $P = 0.008$). For instance, there was a significantly higher percentage of Pd in the mid ($P = 0.014$) and hind ($P = 0.029$) intestine compared to the anterior intestine. The number of PS-Pd NPs found in the muscularis represent 9.37, 3.05 and 3.15% of the total mass found in all gut layers (Fig. 3) in the anterior, mid and hind intestine respectively. Similarly, there were some statistical differences within the percentage of Pd in the muscularis (Kruskal-Wallis, H = 9.722, DF = 2, $P = 0.008$), with the anterior intestine having significantly more compared to both the mid ($P = 0.014$) and hind ($P = 0.029$), respectively. The presence of PS-Pd NPs in the serosal saline was found only in the anterior intestine, with 0.63 ± 0.33 % of the tissue Pd entering this compartment (Fig. 3).

### 3.3. Number of PS-Pd NPs in the gut tissue

The gut epithelium is made of several different layers and each was assessed for the number of particles found. After the 4 h exposure, PS-Pd NPs were found in all tissue layers (mucosa, muscularis and serosal saline) of each intestinal region, with a combined total of $216 \times 10^6 \pm 40 \times 10^6$, $262 \times 10^6 \pm 22 \times 10^6$ and 720 x$10^6 \pm 251 \times 10^6$

**Table 1**
The moisture content (%) and fluid flux (μL $cm^{-2}h^{-1}$) of the regions of the gastrointestinal tract.

| Measurement | Control | PS-Pd NPs |
|---|---|---|
| Moisture content (%) | | |
| Anterior mucosa | 73.0 ± 3.1 | 76.3 ± 1.7 |
| Anterior muscularis | 79.6 ± 3.7 | 76.6 ± 0.4 |
| Mid intestine mucosa | 85.0 ± 1.6 | 85.9 ± 0.9 |
| Mid intestine muscularis | 73.0 ± 1.3 | 74.9 ± 1.3 |
| Hind intestine mucosa | 86.6 ± 1.4 | 87.7 ± 0.9 |
| Hind intestine muscularis | 80.3 ± 3.5 | 78.4 ± 0.8 |
| Fluid flux (μL $cm^{-2}h^{-1}$) | | |
| Anterior intestine | −65.6 ± 48.0 | −20.4 ± 8.4 |
| Mid intestine | −2.6 ± 0.5 | 0.0 ± 0.3 |
| Hind intestine | 7.5 ± 1.5 | 4.5 ± 2.0 |

Data are mean ± SEM (n = 6). Note there was no significant difference between the moisture content and fluid flux treatments.

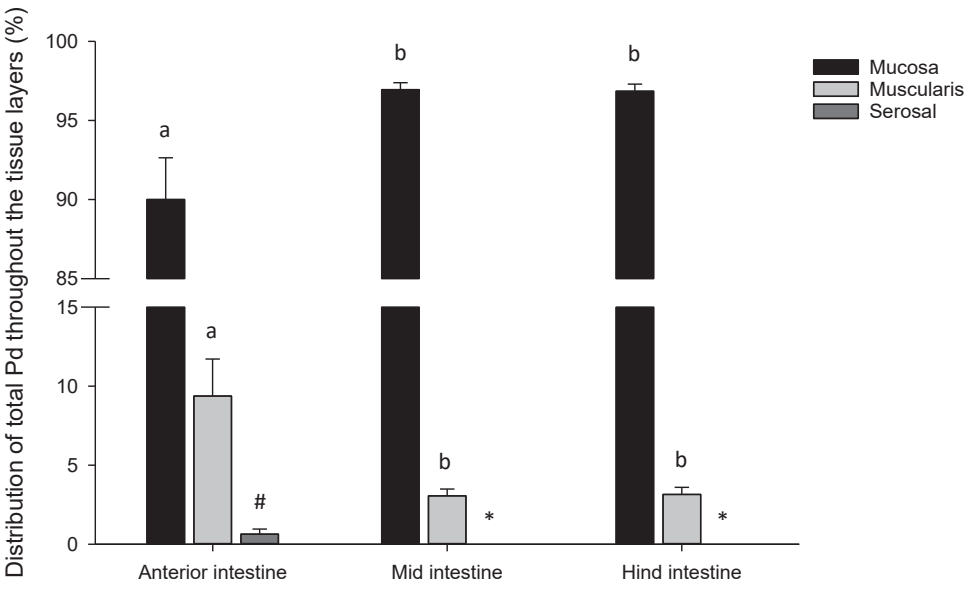


**Fig. 3.** Distribution of total palladium found through the layers of the gastrointestinal tract following exposure to a control or 1 mg Pd $L^{-1}$ as PS-Pd NPs. Data are mean ± S.E.M., n = 5/6. Different lower case letters denote significant difference between gut region, but within the same tissue type. (#) denotes significant difference between anterior intestine serosal saline compared to other gut regions (*) denotes no detectable PS-Pd NPs found in the serosal saline of the mid and hind intestine. Note: the total Pd found in the controls was below the limit of detection (<0.24 ng). Percent Pd = (mass in tissue layer/total Pd in the 3 layers of that gut region) × 100. The anterior serosal saline particle mass concentration was calculated directly through spICP-MS.

(mean ± SEM, n = 6, Fig. 4) particles in the anterior, mid and hind intestine regions, respectively. While the hind intestine had a 3.3 and 2.7-fold higher number of particles compared the anterior and mid intestine respectively, there was no significant difference between these tissues (Kruskal-Wallis, H = 5.345, DF = 2, $P = 0.069$).

The inner most layer of the gut epithelium is the mucosa, and this is the first layer the PS-Pd NPs encounter. Most of the particles taken up by the gut were in the mucosa (Fig. 4), with a total of 197 $x10^6$ ± 38 $x10^6$, 255 $x10^6$ ± 22 $x10^6$ and 697 $x10^6$ ± 246 $x10^6$ (mean ± SEM, n = 6) particles in the anterior intestine, mid intestine and hind intestine, respectively. Despite the hind intestine containing 3.5 and 2.7-fold higher number of particles, there were no statistically significant differences in the number of particles found in the mucosa between each gut region (Kruskal-Wallis, H = 5.135, DF = 2, $P = 0.077$). In terms of total Pd tissue concentrations, this equates to 713 ± 169, 2737 ± 494 and 2792 ± 833 ng Pd $g^{-1}$ (mean ± SEM, n = 6) in the anterior, mid and hind intestine mucosa, respectively (Fig. 5). There were some statistical differences in the mucosa total Pd concentrations (one-way ANOVA, F = 8.304, DF = 2, $P = 0.004$), with the anterior being significantly less compared to both the mid ($P = 0.005$) and hind intestine ($P = 0.014$).

Passage across the mucosa leads to the muscularis layer of the gut epithelium. Movement into this layer is time-dependent and as such fewer particles were found in this layer compared to the mucosa (Fig. 4). Even so, PS-Pd NPs were able to pass into the muscularis. A total of 18 $x10^6$ ± 3 $x10^6$, 8 $x10^6$ ± 1 $x10^6$ and 23 $x10^6$ ± 5 $x10^6$ (mean ± SEM, n = 6) particles were found in the anterior, mid and hind intestine muscularis, respectively, with some regional effects observed (one-way ANOVA, F = 5.286, DF = 2, $P = 0.018$). For instance, the mid intestine had significantly fewer particles compared to the hind intestine ($P = 0.016$). The anterior intestine did not significantly differ compared to any other gut region (mid and hind intestine $P = 0.112$ and 0.572, respectively). In terms of total Pd tissue concentration, this equates to 58.7 ± 12.3, 55.2 ± 4.8 and 103.9 ± 19.0 ng $g^{-1}$ (mean ± SEM, n = 6) in the anterior, mid and hind intestine mucosa, respectively (Fig. 5), with no significant difference between gut regions (one-way ANOVA, F = 4.136, DF = 2, $P = 0.037$, Tukey's $P = 0.052$–0.981).

Crossing the muscularis and into the serosal saline indicates transepithelial uptake through the intestinal barrier from the gut lumen to the tissue. The mass concentration of PS-Pd NPs found in this fluid compartment were 0.011 ± 0.004 ng $mL^{-1}$ equating to 6.90 × $10^5$ ± 3.25 $x10^5$ (mean ± SEM, n = 6, Fig. 4) nanoplastic particles that enter the fish tissue.

### 3.4. Relative absorption of PS-Pd NPs into the gut sac

The total number of PS-Pd NPs introduced into the gut lumen of the anterior, mid and hind intestine at the start of the experiment was 9.98, 3.87 and 7.26 $x10^9$ (mean ± SEM, n = 6) particles, respectively. The amount of PS-Pd NPs that were taken up into the tissue, relative to the amount added to the gut lumen (on a mass balance) in the anterior, mid and hind intestine was 2.5 ± 0.2, 6.8 ± 0.2 and 9.4 ± 0.3 % (mean ± SEM, n = 6, Fig. 6), respectively. This percentage of accumulated nanoplastics into the tissues showed some significant differences between regions (Krukal-Wallis, H = 7.906, DF = 2, $P = 0.019$). Both the mid intestine ($P = 0.034$) and hind intestine ($P = 0.046$) accumulated a higher percentage from the gut lumen compared to the anterior intestine (Fig. 6). However, there was no significant difference between the mid and hind intestine ($P = 0.994$).

## 4. Discussion

This study is the first to demonstrate the capacity for nanoplastics to translocate out of the fish gut lumen. Together, all tissue layers (mucosa, muscularis and serosal saline) in all gut regions (anterior-, mid and hind-intestine) accumulated a total of 1.20 ± 0.27 $x10^9$ particles in as little as 4 h, representing 2.5–9.4% of those added to the gut lumen at the start of the experiment. The highest accumulation, as evidenced by PS-Pd NP appearance in the serosal saline (e.g., blood supply), was from the anterior intestine, whereby as many as 700,000 particles (0.6% of those that entered the tissue) passed through the intestinal barrier (mucosa and muscularis). These nanoplastics then have the potential to distribute throughout the fish body via the blood supply and potentially accumulate in the internal organs. Consequently, it is these plastics that have the potential to cause direct internal toxicological damage and transfer through the food chain.

Previous studies have investigated the bioaccumulation and effects of nanoplastics with lower trophic levels, including bacteria (Fringer et al., 2020), algae (Bhattacharya et al., 2010), various invertebrates (e.g., earthworms (Lahive et al., 2021), *Daphnia* (Ma et al., 2016), *gammarus pulex* (Redondo-Hasselerharm et al., 2021), and shellfish (Al-Sid-Cheikh et al., 2018)), as well as with fish species (Guimarães et al., 2021; Van Pomeren et al., 2017). Generalising across studies is difficult because of variation in methodology, but nanoplastics when compared to microplastics at the corresponding mass concentration, show a tendency towards greater accumulation potential and increased biological

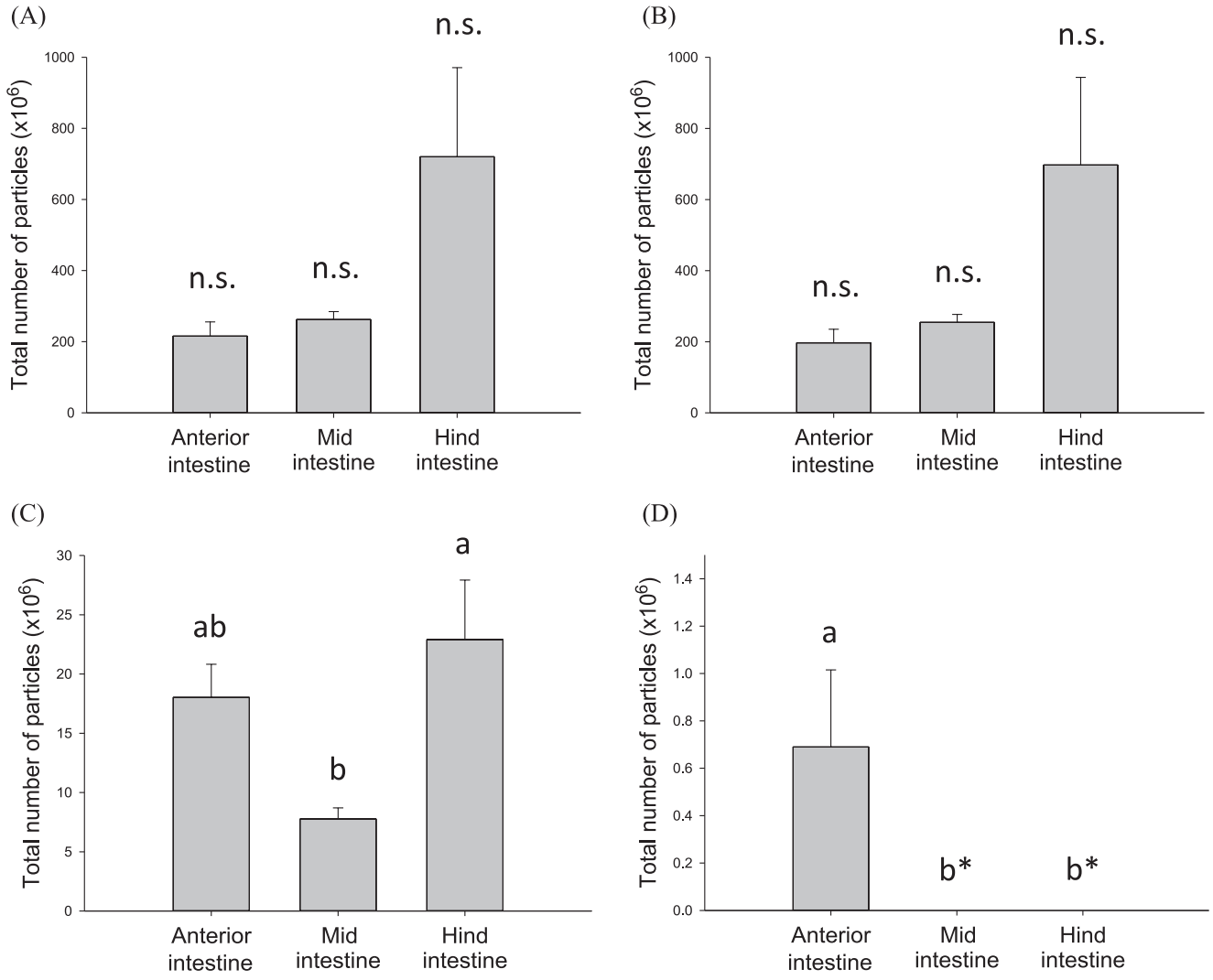


**Fig. 4.** Total number of particles present in the (A) whole gut sac, (B) mucosa, (C) muscularis, and (D) serosal saline. Data are mean ± S.E.M. (n = 6). Different lower case letters denote significant difference between gut regions, but within the same tissue type. (n.s.) denotes no significant difference between gut regions. (n.s.) denotes no significant difference between gut regions. (*) denotes no detectable PS-Pd NPs found in the serosal saline of the mid and hind intestine. Note 1 ng of Pd as PS-Pd NPs equates to $10.3 \pm 0.5 \times 10^6$ particles, and was used to calculate the number of particles present in the mucosa and muscularis. The number of particles in the anterior intestine serosal saline was measured directly by spICP-MS.

impact owing to their smaller size, mass to surface ratio and other inherent properties of the nanoscale (Klaine et al., 2012; Mattsson et al., 2017). Thus, the hazard of nano-sized particles is increased since they are able to pass through biological barriers through endocytosis pathways, penetrate tissue and accumulate in organs. Our study further demonstrates the passage through the intestinal barrier within the *ex vivo* gut sac model quantifying the proportion of nanoplastics that may gain entry to the wider biological system following uptake. The 700,000 nanoplastics, representing 0.6% of those taken up by the anterior intestine, are free to enter the blood stream and circulate through the fish body may have two main consequences: 1) invoking toxic responses in the fish themselves, and 2) further trophic transfer. However, there is limited information on both these possibilities. Zebrafish embryos exposed to polystyrene nanoplastics exhibited particle uptake following ingestion and the distribution and localization of nanoplastics to the eyes (Van Pomeren et al., 2017). Amino-modified polystyrene nanoplastics of up to 330 nm were able to cross the blood brain barrier of crucian carp following introduction via a zooplankton diet resulting in brain damage and behavioural effects in the fish (Mattsson et al., 2017). The presence of nanoplastics in fish carcass tissue is highly plausible since microplastics have been found in wild caught fish which contained mean concentrations of 0.51, 0.25 and 1.26 particles per gram of fish carcass tissue (Zitouni et al., 2020).

The exposure of humans to microplastics is well established through inhalation (Gasperi et al., 2018), and ingestion via a wide variety of food items, including table salt, sugar, honey, alcohol and seafood (see review by Cox et al., 2019). As with biota, the fate of such plastic items is not fully understood, but high-profile cases such as the finding of microplastics in human placenta (Ragusa et al., 2021) have heightened the concern of exposure. The ingestion of nanoplastics may be of even greater concern given their propensity to cross biological membranes. Plastics carry with them endogenous chemicals that are added to the polymer resin during the manufacturing process (Caruso 2019). These include known toxicants such as endocrine disruptors, persistent organic chemicals or trace metals which have been shown to become bioavailable following release from plastic *in vivo* (Boyle et al., 2020a; Lehner et al., 2019). The increased risk of chemicals associated to nanoplastics, as opposed to microplastics, again relates to their ability for cellular internalization meaning that such chemicals could be released in proximity to sites of cellular functioning and induce toxicity (Lehner et al., 2019).

In humans, the passage of titanium dioxide particles (*in vivo*) reaches

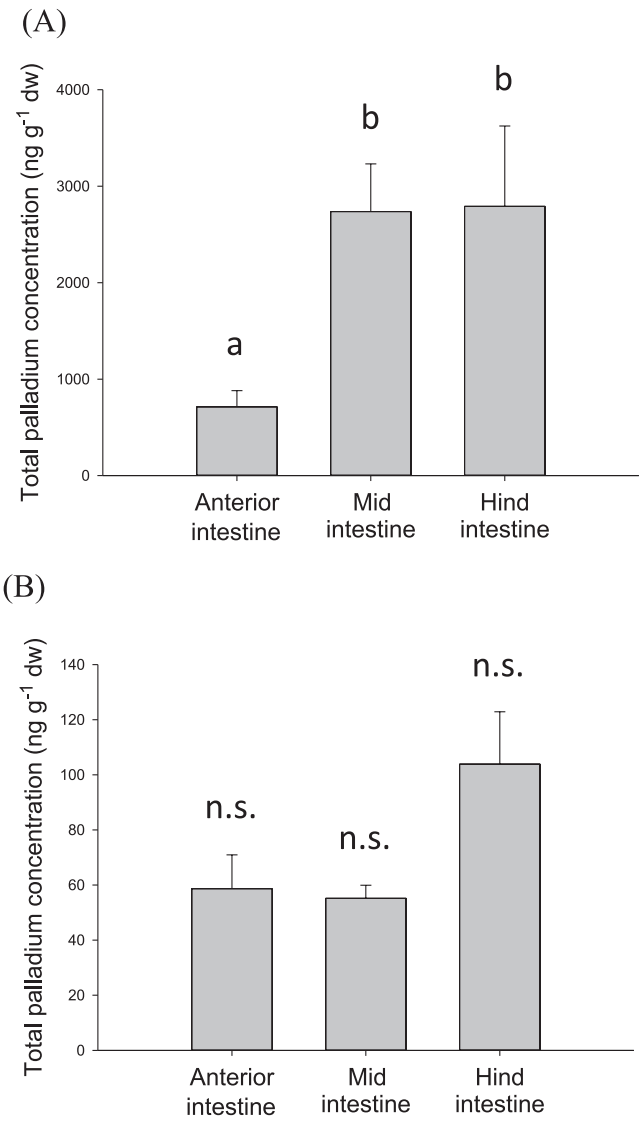


**Fig. 5.** Gastrointestinal tract tissue total palladium concentrations (ng $g^{-1}$ dw) in the mucosa (A) or muscularis (B). Data are mean ± S.E.M. (n = 6). Different lower case letters denote significant difference between gut regions. (n.s.) denotes no significant difference between gut regions. The limit of detection was 6 ± 2 ng $g^{-1}$, and the control samples remained below this (mean ± SEM, n = 24). Note 1 ng of Pd as PS-Pd NPs equates to 10.3 ± 0.5 × $10^6$ particles to derive tissue particle number concentrations.

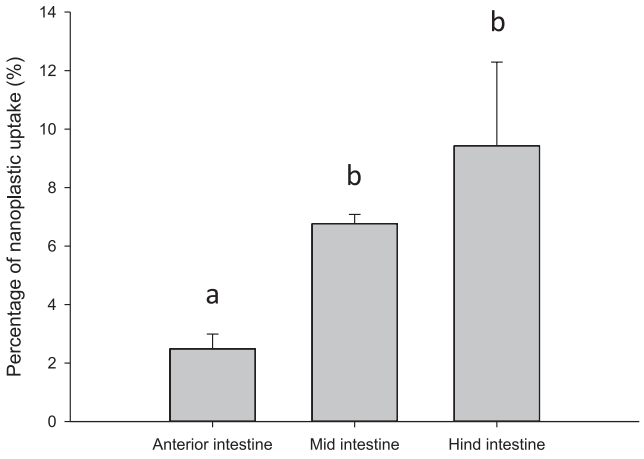


**Fig. 6.** The relative amount of PS-Pd NPs absorbed by the gastrointestinal tract. Data are mean ± SEM (n = 6). Different lower case letters denote significant difference between gut regions.

a maximum after 6 h (Pele et al., 2015). Indeed, fish body temperatures are >20 °C lower than mammals, resulting in slower uptake dynamics, including uptake of particles (Clark et al., 2019b; Clark et al., 2020). Therefore, at the time of sampling after 4 h, the PS-Pd NPs could be in the process of passing between the muscularis and serosal saline, thereby underestimating the number of nanoplastics that could enter the blood supply. This is in contrast to the low/negligible tissue accumulation from direct feeding (Batel et al., 2020) or incidental ingestion (Avio et al., 2015) of microplastics. Clearly, the potential for microplastic accumulation from the gastrointestinal tract appears limited, yet the data here supports the idea that nanoplastics are more bioavailable, potentially due to the smaller size of the latter. However, the environmental water concentrations of nanoplastics are predicted to be in the low μg $L^{-1}$ range (Al-Sid-Cheikh et al., 2018).

In the present study, PS-Pd NPs showed a similar percentage of accumulation from the gut lumen of freshwater fish as other nano-sized particles of anthropogenic origin (i.e., metal-containing engineered nanomaterials (Clark et al., 2019b)). However, particle presence in the serosal saline were not previously observed (Clark et al., 2019b). The 0.6% of the nanoplastics accumulated that were found in the serosal saline following the PS-Pd NP exposure was also higher than that found from copper nanoparticles (0.1% (Boyle et al., 2020b)). The PS-Pd NPs can be accumulated in the pyloric caeca as this region shows evidence of translocating bacteria through endocytosis (Ringø et al., 2007), the mechanism associated with nanoparticle uptake. While endocytosis is rate-limited, from the present data, it is not possible to determine if the gastrointestinal tract has reached saturation for uptake, or, given more time, if more PS-Pd NPs would pass into the serosal saline. Conceivably, the latter scenario is likely suggesting that our finding that nanoplastics cross the intestinal barrier is an underestimation both on account of piscine digestive physiology and the limitations of the gut sac method. Conversely, the concentration of PS-Pd NPs introduced into the gut sacs is a higher dose than a fish may encounter in the wild and the aggregation of nanoplastics that may occur in the environment prior to ingestion may result in nanoplastics being unable to cross the gut barrier. Such considerations are needed when attempting to extrapolate these experimental findings to natural settings, but nonetheless our study provides a demonstration for the uptake of nanoplastics from the gut lumen to the tissue.

The use of 4 h in the present study is the length of time that an *ex vivo* gut sac maintains viability and functionality. However, the *in vivo* exposure time within the gut lumen of the fish will depend on the residence time of food. The longer the residence time, the longer the exposure, and hence a greater likelihood of internal tissue accumulation. In some fish species, the residence time is as much as 10–20 h (*Solea senegalensis* and *Spratus aurata*, Gilannejad et al., 2019). Therefore, *in vivo* exposures may have longer exposure conditions in the intestine that allow for higher gut uptake into internal tissues. In addition, the physiological gut saline used here was fixed in salt content and pH, both of which change throughout the gastrointestinal tract. In addition, both are known variables to induce changes in behaviour of nanoparticles (Lead et al., 2018), including nanoplastics (e.g., Fig. 2), with changes in bioavailability, mainly the larger the particles becoming less bioavailable. Another key difference to *in vivo* conditions is the presence of food in the lumen of the gastrointestinal tract, which can alter the bioavailability of chemicals and particles. The gut sac experiment uses a saline representative of the gut lumen, with no organic material representing food. The amount accumulated from the gut is reduced in the presence of food, for example, when one feeds a fish a diet containing dissolved metals or inorganic engineered nanoparticles (Clark et al., 2019a). The gut sac can show an absorption efficiency of up to 20% for these materials (Clark et al., 2019b), but *in vivo* only 3% can enter the fish (Clark

et al., 2019a). Regardless, the gut sac demonstrates the ability of the gut to accumulate and pass such materials.

## 5. Conclusions

In summary, our study provides the first quantitative assessment of the potential uptake of nanoplastics by the fish gut. The fast method of uptake using the gut sac technique provides evidence for further investigation using labelled nanoplastics techniques to understand the potential environmental hazards of these materials. This raises questions surrounding the potential trophic transfer of nanoplastics, including to humans. Further investigation should involve an *in vivo* exposure to the gastrointestinal tract through incorporation into the diet to assess for target organs (e.g., carcass and associated human health risk), and any effects on the gut itself or internal organs.

### *CRediT authorship contribution statement*

**Nathaniel J. Clark:** Conceptualization, Methodology, Validation, Formal analysis, Investigation, Writing – original draft. **Farhan R. Khan:** Conceptualization, Methodology, Investigation, Writing – original draft. **Denise M. Mitrano:** Conceptualization, Methodology, Resources, Writing – original draft. **David Boyle:** Conceptualization, Methodology, Writing – review & editing. **Richard C. Thompson:** Resources, Writing – review & editing, Supervision, Funding acquisition.

### Declaration of Competing Interest

The authors declare that they have no known competing financial interests or personal relationships that could have appeared to influence the work reported in this paper.

### Acknowledgements

N.J.C. and R.C.T. were funded by the NERC Current and Future Effects of Microplastics on Marine Ecosystems (MINIMISE) project, reference NE/S003967/1. F.R.K. was part funded by MarinePlastic (Velux Fonden). D.M.M. was funded by the Swiss National Science Foundation, Project number PCEFP2_186856. The authors would like to thank Ben Eynon for husbandry support and Dr Rob Clough for ICP-MS support. The datasets generated during and/or analysed during the current study are available from the corresponding author on reasonable request.

### References

Al-Jubory, A.R., Handy, R.D., 2013. Uptake of titanium from TiO2 nanoparticle exposure in the isolated perfused intestine of rainbow trout: nystatin, vanadate and novel CO2-sensitive components. Nanotoxicology 7 (8), 1282–1301.

Al-Sid-Cheikh, M., Rowland, S.J., Kaegi, R., Henry, T.B., Cormier, M.-A., Thompson, R.C., 2020. Synthesis of 14 C-labelled polystyrene nanoplastics for environmental studies. Commun. Mater. 1, 1–8.

Al-Sid-Cheikh, M., Rowland, S.J., Stevenson, K., Rouleau, C., Henry, T.B., Thompson, R. C., 2018. Uptake, whole-body distribution, and depuration of nanoplastics by the scallop pecten maximus at environmentally realistic concentrations. Environ. Sci. Technol. 52 (24), 14480–14486.

Arthur, C., Baker, J.E., Bamford, H.A., 2009. Proceedings of the International Research Workshop on the Occurrence, Effects, and Fate of Microplastic Marine Debris. University of Washington Tacoma, Tacoma, WA, USA.

Avio, C.G., Gorbi, S., Regoli, F., 2015. Experimental development of a new protocol for extraction and characterization of microplastics in fish tissues: first observations in commercial species from Adriatic Sea. Mar. Environ. Res. 111, 18–26.

Azevedo-Santos, V.M., Gonçalves, G.R.L., Manoel, P.S., Andrade, M.C., Lima, F.P., Pelicice, F.M., 2019. Plastic ingestion by fish: A global assessment. Environ. Pollution (Barking, Essex 1987) 255, 112994. https://doi.org/10.1016/j.envpol.2019.112994.

Barnes, D.K.A., Galgani, F., Thompson, R.C., Barlaz, M., 2009. Accumulation and fragmentation of plastic debris in global environments. Philos. Trans. Royal Soc. B: Biol. Sci. 364 (1526), 1985–1998.

Batel, A., Baumann, L., Carteny, C.C., Cormier, B., Keiter, S.H., Braunbeck, T., 2020. Histological, enzymatic and chemical analyses of the potential effects of differently sized microplastic particles upon long-term ingestion in zebrafish (*Danio rerio*). Mar. Pollut. Bull. 153, 111022. https://doi.org/10.1016/j.marpolbul.2020.111022.

Bhattacharya, P., Lin, S., Turner, J.P., Ke, P.C., 2010. Physical adsorption of charged plastic nanoparticles affects algal photosynthesis. J. Phys. Chem. C 114 (39), 16556–16561.

Boyle, D., Catarino, A.I., Clark, N.J., Henry, T.B., 2020a. Polyvinyl chloride (PVC) plastic fragments release Pb additives that are bioavailable in zebrafish. Environ. Pollut. 263, 114422. https://doi.org/10.1016/j.envpol.2020.114422.

Boyle, D., Clark, N.J., Botha, T.L., Handy, R.D., 2020b. Comparison of the dietary bioavailability of copper sulphate and copper oxide nanomaterials in *ex vivo* gut sacs of rainbow trout: effects of low pH and amino acids in the lumen. Environ. Sci. Nano 7 (7), 1967–1979.

Bury, N.R., Grosell, M., Wood, C., Hogstrand, C., Wilson, R., Rankin, J.C., Busk, M., Lecklin, T., Jensen, F.B., 2001. Intestinal iron uptake in the European flounder (*Platichthys flesus*). J. Exp. Biol. 204, 3779–3787.

Caruso, G., 2019. Microplastics as vectors of contaminants. Mar. Pollut. Bull. 146, 921–924.

Catarino, A.I., Frutos, A., Henry, T.B., 2019. Use of fluorescent-labelled nanoplastics (NPs) to demonstrate NP absorption is inconclusive without adequate controls. Sci. Total Environ. 670, 915–920.

Chain, E.P.o.C.i.t.F. Presence of microplastics and nanoplastics in food, with particular focus on seafood. Efsa J. 2016;14:e04501.

Clark, N.J., Boyle, D., Eynon, B.P., Handy, R.D., 2019a. Dietary exposure to silver nitrate compared to two forms of silver nanoparticles in rainbow trout: bioaccumulation potential with minimal physiological effects. Environ. Sci. Nano 6 (5), 1393–1405.

Clark, N.J., Boyle, D., Handy, R.D., 2019b. An assessment of the dietary bioavailability of silver nanomaterials in rainbow trout using an *ex vivo* gut sac technique. Environ. Sci. Nano 6 (2), 646–660.

Clark, N.J., Clough, R., Boyle, D., Handy, R.D., 2019c. Development of a suitable detection method for silver nanoparticles in fish tissue using single particle ICP-MS. Environ. Sci.-Nano 6 (11), 3388–3400.

Clark, N.J., Woznica, W., Handy, R.D., 2020. Dietary bioaccumulation potential of silver nanomaterials compared to silver nitrate in wistar rats using an *ex vivo* gut sac technique. Ecotoxicol. Environ. Saf. 200, 110745. https://doi.org/10.1016/j.ecoenv.2020.110745.

Cox, K.D., Covernton, G.A., Davies, H.L., Dower, J.F., Juanes, F., Dudas, S.E., 2019. Human consumption of microplastics. Environ. Sci. Technol. 53 (12), 7068–7074.

Fringer, V.S., Fawcett, L.P., Mitrano, D.M., Maurer-Jones, M.A., 2020. Impacts of nanoplastics on the viability and riboflavin secretion in the model bacteria *Shewanella oneidensis*. Front. Environ. Sci. 8 https://doi.org/10.3389/fenvs.2020.0009710.3389/fenvs.2020.00097.s001.

Gasperi, J., Wright, S.L., Dris, R., Collard, F., Mandin, C., Guerrouache, M., Langlois, V., Kelly, F.J., Tassin, B., 2018. Microplastics in air: are we breathing it in? Curr. Opin. Environ. Sci. Health 1, 1–5.

Gigault, J., El Hadri, H., Nguyen, B., Grassl, B., Rowenczyk, L., Tufenkji, N., Feng, S., Wiesner, M., 2021. Nanoplastics are neither microplastics nor engineered nanoparticles. Nat. Nanotechnol. 16 (5), 501–507.

Gilannejad, N., Silva, T., Martínez-Rodríguez, G., Yúfera, M., 2019. Effect of feeding time and frequency on gut transit and feed digestibility in two fish species with different feeding behaviours, gilthead seabream and Senegalese sole. Aquaculture 513, 734438. https://doi.org/10.1016/j.aquaculture.2019.734438.

Guimarães, A.T.B., Estrela, F.N., Pereira, P.S., de Andrade Vieira, J.E., de Lima Rodrigues, A.S., Silva, F.G., Malafaia, G., 2021. Toxicity of polystyrene nanoplastics in *Ctenopharyngodon idella* juveniles: a genotoxic, mutagenic and cytotoxic perspective. Sci. Total Environ. 752:141937.

Kershaw, P., 2015. Sources, fate and effects of microplastics in the marine environment: a global assessment. International Maritime Organization.

Khan, F.R., Boyle, D., Chang, E., Bury, N.R., 2017. Do polyethylene microplastic beads alter the intestinal uptake of Ag in rainbow trout (*Oncorhynchus mykiss*)? Analysis of the MP vector effect using in vitro gut sacs. Environ. Pollut. 231, 200–206.

Klaine, S.J., Koelmans, A.A., Horne, N., Carley, S., Handy, R.D., Kapustka, L., Nowack, B., von der Kammer, F., 2012. Paradigms to assess the environmental impact of manufactured nanomaterials. Environ. Toxicol. Chem. 31, 3–14.

Koelmans, A.A., Besseling, E., Shim, W.J., 2015. Nanoplastics in the aquatic environment. Critical review. Mar. Anthropogenic Litter 325-340.

Lahive, E., Cross, R., Saarloos, A.I., Horton, A.A., Svendsen, C., Hufenus, R., Mitrano, D. M., 2021. Earthworms ingest microplastic fibres and nanoplastics with effects on egestion rate and long-term retention. Sci. Total Environ. 151022. https://doi.org/10.1016/j.scitotenv.2021.151022.

Lead, J.R., Batley, G.E., Alvarez, P.J.J., Croteau, M.-N., Handy, R.D., McLaughlin, M.J., Judy, J.D., Schirmer, K., 2018. Nanomaterials in the environment: Behavior, fate, bioavailability, and effects-An updated review. Environ. Toxicol. Chem. 37 (8), 2029–2063.

Lehner, R., Weder, C., Petri-Fink, A., Rothen-Rutishauser, B., 2019. Emergence of nanoplastic in the environment and possible impact on human health. Environ. Sci. Technol. 53 (4), 1748–1765.

Lusher, A., Hollman, P., Mendoza-Hill, J., 2017. Microplastics in fisheries and aquaculture: status of knowledge on their occurrence and implications for aquatic organisms and food safety. FAO.

Ma, Y., Huang, A., Cao, S., Sun, F., Wang, L., Guo, H., Ji, R., 2016. Effects of nanoplastics and microplastics on toxicity, bioaccumulation, and environmental fate of phenanthrene in fresh water. Environ. Pollut. 219, 166–173.

Mattsson, K., Johnson, E.V., Malmendal, A., Linse, S., Hansson, L.-A., Cedervall, T., 2017. Brain damage and behavioural disorders in fish induced by plastic nanoparticles delivered through the food chain. Sci. Rep. 7, 1–7.

Mitrano, D.M., Beltzung, A., Frehland, S., Schmiedgruber, M., Cingolani, A., Schmidt, F., 2019. Synthesis of metal-doped nanoplastics and their utility to investigate fate and behaviour in complex environmental systems. Nat. Nanotechnol. 14 (4), 362–368.

Mitrano, D.M., Wick, P., Nowack, B., 2021. Placing nanoplastics in the context of global plastic pollution. Nat. Nanotechnol. 16 (5), 491–500.
Ojo, A.A., Wood, C.M., 2007. In vitro analysis of the bioavailability of six metals via the gastro-intestinal tract of the rainbow trout (*Oncorhynchus mykiss*). Aquat. Toxicol. 83 (1), 10–23.
Pace, H.E., Rogers, N.J., Jarolimek, C., Coleman, V.A., Higgins, C.P., Ranville, J.F., 2011. Determining transport efficiency for the purpose of counting and sizing nanoparticles via single particle inductively coupled plasma mass spectrometry. Anal. Chem. 83 (24), 9361–9369.
Pele, L.C., Thoree, V., Bruggraber, S.F., Koller, D., Thompson, R.P., Lomer, M.C., Powell, J.J., 2015. Pharmaceutical/food grade titanium dioxide particles are absorbed into the bloodstream of human volunteers. Part. Fibre Toxicol. 12, 26.
Peters, R.J.B., Rivera, Z.H., van Bemmel, G., Marvin, H.J.P., Weigel, S., Bouwmeester, H., 2014. Development and validation of single particle ICP-MS for sizing and quantitative determination of nano-silver in chicken meat. Anal. Bioanal. Chem. 406, 3875–3885.
Phuong, N.N., Zalouk-Vergnoux, A., Poirier, L., Kamari, A., Châtel, A., Mouneyrac, C., Lagarde, F., 2016. Is there any consistency between the microplastics found in the field and those used in laboratory experiments? Environ. Pollut. 211, 111–123.
Ragusa, A., Svelato, A., Santacroce, C., Catalano, P., Notarstefano, V., Carnevali, O., Papa, F., Rongioletti, M.C.A., Baiocco, F., Draghi, S., D'Amore, E., Rinaldo, D., Matta, M., Giorgini, E., 2021. Plasticenta: First evidence of microplastics in human placenta. Environ. Int. 146, 106274. https://doi.org/10.1016/j.envint.2020.106274.
Ramsperger, A., Narayana, V.K.B., Groß, W., Mohanraj, J., Thelakkat, M., Greiner, A., Schmalz, H., Kress, H., Laforsch, C., 2020. Environmental exposure enhances the internalization of microplastic particles into cells. Sci. Adv. 6:eabd1211.
Redondo-Hasselerharm, P.E., Vink, G., Mitrano, D.M., Koelmans, A.A., 2021. Metal-doping of nanoplastics enables accurate assessment of uptake and effects on Gammarus pulex. Environ. Sci. Nano 8 (6), 1761–1770.
Ringø, E., Myklebust, R., Mayhew, T.M., Olsen, R.E., 2007. Bacterial translocation and pathogenesis in the digestive tract of larvae and fry. Aquaculture 268 (1-4), 251–264.
Shen, M., Zhang, Y., Zhu, Y., Song, B., Zeng, G., Hu, D., Wen, X., Ren, X., 2019. Recent advances in toxicological research of nanoplastics in the environment: A review. Environ. Pollut. 252, 511–521.
van Pomeren, M., Brun, N.R., Peijnenburg, W.J.G.M., Vijver, M.G., 2017. Exploring uptake and biodistribution of polystyrene (nano) particles in zebrafish embryos at different developmental stages. Aquat. Toxicol. 190, 40–45.
Whittamore, J.M., Genz, J., Grosell, M., Wilson, R.W., 2016. Measuring intestinal fluid transport in vitro: Gravimetric method versus non-absorbable marker. Comp. Biochem. Physiol. A: Mol. Integr. Physiol. 194, 27–36.
Zalasiewicz, J., Waters, C.N., Ivar do Sul, J.A., Corcoran, P.L., Barnosky, A.D., Cearreta, A., Edgeworth, M., Gałuszka, A., Jeandel, C., Leinfelder, R., McNeill, J.R., Steffen, W., Summerhayes, C., Wagreich, M., Williams, M., Wolfe, A.P., Yonan, Y., 2016. The geological cycle of plastics and their use as a stratigraphic indicator of the Anthropocene. Anthropocene 13, 4–17.
Zitouni, N., Bousserrhine, N., Belbekhouche, S., Missawi, O., Alphonse, V., Boughatass, I., Banni, M., 2020. First report on the presence of small microplastics ($\leq$ 3 μm) in tissue of the commercial fish Serranus scriba (Linnaeus. 1758) from Tunisian coasts and associated cellular alterations. Environ. Pollut. 263:114576.